## Title

X-RAY PHOTOEMESSION MOLECULAR ORBITALS OF HYDROGEN FLUORIDE AND THE FLUORINATED METHANES



## Authors

Banna, M.S.
Mills, B.E.
Davis, D.W.
et al.

## Publication Date

1974-06-01

Submitted to Journal of
Chemical Physics

LBL-2930
Preprint



# X-RAY PHOTOEMISSION MOLECULAR ORBITALS OF HYDROGEN FLUORIDE AND THE FLUORINATED METHANES

M. S. Banna, B. E. Mills, D. W. Davis,
and D. A. Shirley

June 1974

Prepared for the U. S. Atomic Energy Commission
under Contract W-7405-ENG-48



## DISCLAIMER

# X-RAY PHOTOEMISSION MOLECULAR ORBITALS OF HYDROGEN FLUORIDE AND THE FLUORINATED METHANES*

M. S. Banna, B. E. Mills, D. W. Davis, and D. A. Shirley

Department of Chemistry and
Lawrence Berkeley Laboratory
University of California
Berkeley, California 94720

June 1974

## ABSTRACT

The X-ray photoemission molecular orbital spectra of gaseous hydrogen fluoride and the fluorinated methanes ($CH_nF_{4-n}$, $0 \leq n \leq 4$) are reported. A three-parameter model was used to predict experimental binding energies from ab initio Koopmans' theorem energies. Excellent agreement was obtained. Relative intensities of molecular orbitals were computed using the model of Gelius with both CNDO/2 and ab initio atomic populations. In the case of ab initio results, net populations were found to be superior to gross populations in reproducing the experimental intensities. In most cases the theory predicted intensities quite well. Some trends exhibited by the fluoromethane series are noted.

# I. INTRODUCTION

The development of molecular photoelectron spectroscopy[1,2] has made it possible to establish the binding energies of individual molecular orbitals (MO's). Detailed analyses of spectra can yield further information converning the electronic structure of the molecule. For example, Gelius[3] has proposed that x-ray photoemission (XPS) cross sections of MO's should be given approximately by a sum of atomic orbital (AO) cross sections, weighted according to the contribution of each AO to the MO in question. Thus, if $\psi_i$ represents an MO that can be expressed as a linear combination of atomic orbitals $\phi$,

$$\psi_i = \sum_j C_{ij} \phi_j, \tag{1}$$

the x-ray photoemission cross section $\sigma_j$ is given approximately by

$$\sigma_i(\text{MO}) \cong \sum_j P_{ij} \sigma_j(\text{AO}). \tag{2}$$

Here $P_{ij}$ gives the electron population in AO $\phi_j$ given an electron in MO $\psi_i$. The essential physics behind the validity and usefulness of Eq. (2) arises from the fact that for x-ray energies it is a good approximation to treat the photoelectron final state as a plane wave. In this approximation the dipole matrix element for the transition reduces to an overlap integral between an MO and the plane wave. Thus the plane wave essentially selects out a high-k Fourier component of the initial-state wave function, and the overlap integral has large contributions only near the nuclei, where the curvature of the MO radial wavefunction matches that of the plane wave. It is in this region, dominated by the strong nuclear potential, that the MO may be well-represented

by a sum of AO's and Eq (2) follows approximately from Eq (1). In XPS the photoelectron's de Broglie wavelength is approximately 0.35 Å (using Mg Kα x-rays) or 0.32 Å (with Al Kα x-rays) for initial states in the entire MO region. Of course this argument, and Eq. (2) would not apply to ultraviolet photoemission spectroscopy (UPS) because the longer wavelength of the photoelectron makes the photoelectric cross section sensitive to the curvature of the orbitals in the bonding regions, and because the percentage energy variation over the MO region is large.

A second assumption must be made when the electron populations $P_{ij}$ are expressed in terms of the expansion coefficients $C_{ij}$. The quantities $P_{ij}$ have no unique rigorous meaning, and this step is somewhat arbitrary. Even when ab initio MO calculations are employed, one must decide between "net" or "gross" populations[4] or among other schemes. Further possibilities are introduced by the use of more approximate MO theories.

Irrespective of the details of the particular analysis that is adopted, the Gelius model should have considerable diagnostic value even if Eq. (2) is not completely rigorous. Ideally, a given set of calculated XPS atomic cross-sections $\{\sigma(AO)\}$ and a set of measured XPS MO cross-sections $\{\sigma(MO)\}$, would indicate whether a given set of populations $\{P_{ij}\}$ are consistent with the experiment.

The work reported below was undertaken to acquire some insight into the usefulness of the Gelius model. The fluorinated methanes were chosen as the model system because they have already been studied by UPS and are large enough to be challenging but small enough to be tractable, both spectroscopically and theoretically. The XPS experiments are described in Section II. Comparison of

orbital binding energies with earlier work and with theory are made in Section III. Intensities and spectroscopic assignments for individual molecular species are discussed in Section IV. Trends through the whole series are treated in Section V.

## II. EXPERIMENTAL

Samples were obtained from Matheson Gas Co. and studied in the gas phase with the Berkeley Iron-Free Spectrometer.[5] They were irradiated with Mg $K\alpha_{1,2}$ (1.2536 keV) or Al $K\alpha_{1,2}$ (1.4866 keV) x-rays using sample pressures of 50 to 100 microns. Counts were obtained at kinetic energy increments of ~ 0.33 eV and in some cases (in the region up to 30 eV binding energies) at increments of ~ 0.16 eV. Binding energies were calibrated in one of two ways. In some cases neon was run together with the gas under study and the neon 2s (48.42 eV)[2,6] or the neon 2p (21.59 eV)[2] level was scanned with part of the MO region of the gas in question. In other cases, one of the core levels (F 1s or C 1s) was scanned alternately with the MO region. Then, in a separate run, that core level was referenced to one of the neon valence levels. The two methods gave results in good agreement.

Lorentzian functions were non-linear least-squares fitted to the experimental spectra and used to determine the peak positions and areas. Provision was automatically made in the fitting program for the $K\alpha_3$ and $K\alpha_4$ x-ray satellites at 8.412 eV and 10.142 eV higher kinetic energy than the main $K\alpha_{1,2}$ exciting line. In general, it was found that Lorentzians reproduced the experimental peak shapes better than Gaussians, but this does not imply that lifetime broadening is a dominant contributor to the linewidth, because the spectrometer response function is made up of several contributing factors of similar magnitude, and the composite function is rather well approximated by a Lorentzian.

## III. ORBITAL BINDING ENERGIES

The XPS molecular orbital spectra of HF and the five gases $CH_{4-n}F_n$ ($0 \leq n \leq 4$) are shown in Fig. 1. Except for the $CH_4$ spectrum, which was taken with Al $K\alpha_{1,2}$ radiation (in order to reduce the interference of the $K\alpha_3$ and $K\alpha_4$ satellites), all measurements were made using the Mg $K\alpha_{1,2}$ line. The measured binding energies, $E_B(MO)$, are given in Table I and compared to the vertical binding energies measured by UPS.[7,8] Brundle, Robin, and Basch[8] reported a systematic study of the fluoromethane series using He I and He II radiation. They also tabulated some vertical $E_B$ values obtained by earlier workers. Since there is good agreement on the experimental values of $E_B$ (as distinguished from the interpretations), in the cases for which duplicate values are available from earlier studies, we shall simply refer to the tabulation of Brundle et al.,[8] rather than intercomparing the available UPS results. Our interest here is in comparing our XPS $E_B(MO)$ values with the UPS vertical $E_B(MO)$ results. The agreement between the two sets of values is generally excellent, in most cases within 0.1 or 0.2 eV.

Comparison of experimental $E_B(MO)$ values with theory is less straightforward, because self-consistent field calculations of the molecular ground states yield only the orbital energies, $\varepsilon(MO)$, rather than actual binding energies, $E_B(MO)$, of the molecular orbitals. It is in principle possible to calculate $E_B(MO)$ directly by the $\Delta$(SCF) method, in which one calculates the total energy of each final (hole) state and subtracts the total energy of the ground state. This approach is not generally applicable, however, because of expense and convergence problems, and we shall follow the usual practice in interpreting photoemission spectra, of employing SCF calculations only in the molecular ground state.

Even within this restricted framework there is some freedom of choice, as the level of sophistication of the SCF calculation can vary considerably. We have chosen to compare the experimental energies with theoretical orbital energies obtained by Snyder and Basch[9] from ab initio POLYATOM calculations using Gaussian-type orbitals. We have also made CNDO/2 calculations for comparison. Orbital energies from both calculations are listed in Table I.

For each MO, comparison of the figures in Table I establishes the order

$$E_B(MO) < -\varepsilon(MO)_{\underline{ab\ initio}} < -\varepsilon(MO)_{CNDO/2}.$$

The CNDO/2 approach is known to give unreliable energies, and little further discussion seems warranted here. We note that reduction of the $-\varepsilon_{CNDO/2}$ values by 20% will give energies that agree on the whole fairly well. The level ordering is usually correct, but there are several errors, and energy discrepancies of 2 eV between 0.80 ($-\varepsilon_{CNDO/2}$) and $E_B$ are present in some cases. It would be fruitless to attempt to rationalize the remaining discrepancies because the nature of the CNDO/2 approach makes it difficult to distinguish computational approximations from real physical effects.

In comparing $E_B(MO)$ and $-\varepsilon(MO)_{\underline{ab\ initio}}$ the accuracy of the latter is high enough that most of the difference can realistically be attributed to physical effects. The binding energy and orbital energy are related by

$$E_B(MO) = -\varepsilon(MO) - E_R(MO) + \Delta E(MO)_{corr} + \Delta E(MO)_{rel} . \qquad (3)$$

Here $E_R(MO)$ is the relaxation energy of the final state with a hole in the molecular orbital under study, and $\Delta E(MO)_{corr}$ and $\Delta E(MO)_{rel}$, which may have

either sign, are the excess correlation and relativistic energies in the final state over those in the initial state. We shall neglect these last two terms for lack of a good approximate method of dealing with them, noting that they are usually relatively small (i.e., 1 eV or less) in the cases studied here.

The $E_R$ term is often larger and always positive. It arises because the wavefunctions of the passive electrons relax during photoemission from an N-electron system, lowering the energy of the hole state. This phenomenon is usually discussed in connection with Koopmans' Theorem,[10] which states the approximate equality $E_B(MO) \cong -\varepsilon(MO)$. Since $E_R$ tends to increase with $E_B$, it has become customary to correct for $E_R$ empirically by reducing $-\varepsilon$ by some fixed percentage. Thus, Brundle et al.[8] found that the approximate relation $E_B$ (theo) $\cong 0.92\ (-\varepsilon)$ gave a rather good estimate of binding energies in the fluorinated methanes.

With the increased understanding of atomic and extra-atomic relaxation energies accompanying photoemission that has emerged recently, it appears possible to improve our estimates of $E_B(MO)$ from $\varepsilon(MO)$. The fluorinated-methane molecular-orbital $E_B$ values determined by XPS require a more sophisticated approach and also provide insight as to how it should be developed. The spectrum of each fluorinated species in Fig. 1 includes one or two orbitals with $E_B$ near 40 eV, considerably more tightly bound than the rest. These are the orbitals made up primarily of fluorine 2s functions in the atomic-orbital expansion. Although their eigenstates are irreducible representations of the molecular symmetry groups (hence the splitting into $3a_1$ and $2b_1$ in $CH_2F_2$, etc.), these orbitals are also partially core-like in their behavior. They appear to have $E_R$ values of $\sim$ 6 eV, close to the $E_R$ value of 4.9 eV[11] for the 2s level in $F^-$.

We note also that the $2a_1$ level in HF, which is mostly F 2s in character, shows $E_R$ = 4.2 eV. These "F 2s-like" levels would require a correction of 12-13% to bring $-\epsilon$ in line with $E_B$ in the fluorinated methanes, rather than the 8% used by Brundle et al.[8] for the less tightly-bound orbitals. As a first step in determining whether it might be useful to take AO character into account in correcting $-\epsilon$ values for relaxation, we have listed the quantity

$$\Delta\epsilon_{ai} \equiv -\epsilon_{\underline{ab\ initio}} - E_B(\text{XPS})$$

for each orbital, in Table I. Inspection of these $\Delta\epsilon_{ai}$ values, and comparison with the $\epsilon$ and $E_B$ columns, readily reveals several facts:

1. For each molecule the $\Delta\epsilon$ values for the F 2s-like MO's are much larger than those for the other MO's and $\Delta\epsilon/\epsilon$ is somewhat larger.
2. Within each group of non-F 2s - like orbitals the correlation between $\Delta\epsilon$ and $\epsilon$ is not very strong.
3. For both types of orbital, $\overline{\Delta\epsilon}$ increases with the total number of valence electrons in the molecule, where $\overline{\Delta\epsilon}$ is defined as the average $\Delta\epsilon$ for a given type of orbital in each molecule.

Now parts of both 1 and 3 could be "explained" by assuming $\Delta\epsilon/\epsilon$ constant throughout, but this approach does not satisfy all of 1 and 3, nor does it help with 2. To provide estimates of $E_B$ from $\epsilon$ that are both more accurate and theoretically sounder, we propose below a model for $E_R$ that is based on recent studies[12-14] of the role of relaxation energies in core-level binding energies.

Relaxation energies can be somewhat arbitrarily separated into atomic and extra-atomic contributions,

$$E_R = E_R^a + E_R^{ea} \quad . \tag{4}$$

For core levels the atomic term $E_R^a$ is relatively well-defined, as is the above separation. For molecular orbitals $\psi_i$ given by Eq. (1) a first approximation to $E_R^a$ (MO,i) would be given by

$$E_R^a \text{ (MO,i)} = \sum_j |C_{ij}|^2 E_R^a \text{ (AO,j)} \quad , \tag{5}$$

where $E_R^a$ (AO,j) is the relaxation energy of atomic orbital $\phi_j$. The $E_R^{ea}$ term is more difficult to estimate, but it would be expected to increase with molecular size, in analogy to the core-level case.[13] On the basis of these arguments we propose a three-parameter model for estimating the relaxation energies of all the MO's of the fluorinated methanes. We assume, for simplicity, that all "F 2s-like" orbitals have one mean value of $E_R$, that all other orbitals have another, and that $E_R^{ea}$ is the same for all orbitals within a given molecule, but that it rises linearly with the number of fluorines (this crudely expresses the molecular size dependence). After the $\Delta\varepsilon_{ai}$ values in Table I have been used to adjust parameters, the expressions for $E_R$ are

$$E_R = (4.5 + 0.5\ n)\ \text{eV} \tag{6}$$

for F 2s-like orbitals, and

$$E_R = (1.0 + 0.5\ n)\ \text{eV} \tag{7}$$

for all other orbitals, where n is the number of fluorines. In applying these equations we again assume for simplicity that a given orbital is either entirely, or not at all, F 2s-like, even though there is correlation between the amount of F 2s character and $E_R$ in several orbitals that have small admixtures of 2s

character. With this approach we have estimated the "theoretical" values $E_B(\text{theo}) = -\varepsilon - E_R$ given in Table I. The agreement between $E_B(\text{theo})$ estimated in this way and $E_B(\text{expt})$ is on the whole excellent, as Fig. 2 shows. For the 33 orbitals studied the standard and mean deviations between $E_B(\text{theo})$ and $E_B(\text{expt})$ are 0.48 eV and 0.27 eV, respectively. This figure also shows the marked separation between $E_B$ values of the F 2s-like orbitals and those of the other molecular orbitals in these molecules. We conclude that relaxation corrections of the type described here are both conceptually and pragmatically superior to simply reducing the orbital energies by a constant factor.

## IV. INTENSITIES AND SPECTROSCOPIC ASSIGNMENTS

In order to apply the intensity model outlined above, a knowledge of the relative atomic cross section is needed. Thus, to interpret the fluoromethane data the ratios

$\sigma(C2s)/\sigma(C2p)$ , $\sigma(F2s)/\sigma(F2p)$ and $\sigma(F2s)/\sigma(C2s)$ are

required. Gelius obtained the first of these three quantities from the experimental XPS area ratios of methane ($2a_1$ and $1t_2$) and an ab initio calculation. Similarly, the last ratio was obtained from the $4a_1$ and $3t_2$ levels of $CF_4$. The $\sigma(F2s)/\sigma(F2p)$ ratio was interpolated due to the unavailability of a spectrum of either HF or $F_2$. In our case, the $\sigma(C2s)/\sigma(C2p)$ was similarly calculated from the $2a_1$ and $1t_2$ of methane. However, we chose instead to use the $3a_1$ and $4a_1$ levels of $CH_3F$ for the $\sigma(F2s)/\sigma(C2s)$. The $\sigma(F2s)/\sigma(F2p)$ ratio was obtained from $2\sigma$ and $1\Pi_x$, $1\Pi_y$ orbitals of HF (Fig. 1). Gelius used gross populations in calculating his ratios. Since his model neglects the contributions to the cross section from electrons far from the nuclei, it seems more appropriate to employ net populations instead. We have computed ratios using both types of populations. The results are shown in Table II.

It is clear from Table II that the cross section ratios are not independent of the theoretical method used. Furthermore, it is interesting to note that in the case of the $\sigma(C2s)/\sigma(C2p)$ ratio, the type of population used (net or gross) seems to be more important than the quality of the calculation (semi-empirical or ab initio).

The relative molecular orbital intensities calculated from POLYATOM and CNDO/2 populations (using Eqs. (1) and (2) and the cross section ratios from Table II) are compared with experiment in Table III and are shown as vertical bars (using POLYATOM net populations) in Fig. 1. Their positions have been adjusted to

match those of the experimental peaks. Some fitting of the spectra is shown in Fig. 1. Expanded spectra of the low binding-energy regions of the fluorinated methanes are shown in Fig. 3 (with relative intensity calculated using CNDO/2 populations). Individual spectroscopic assignments are discussed below:

## $CH_4$

It is unfortunate that the $K\alpha_3$ and $K\alpha_4$ satellites of the exciting Mg radiation obscure the $1t_2$ peak in methane. The situation is not quite so bad with Al x-rays because the satellites are farther from the $K\alpha_{1,2}$ line. Nonetheless, this has resulted in a large uncertainty in the $2a_1/1t_2$ area ratio. In Fig. 1 the $1t_2$ region of the Al $K\alpha_{1,2}$ XPS spectrum is reproduced using a Jahn-Teller splitting of 0.8 eV and a 2 to 1 intensity ratio of the Jahn-Teller components[15]. These are the values seen in UPS studies[8].

## $CH_3F$

The ordering of $5a_1$ and 1e has been uncertain. Both CNDO and POLYATOM yield a lower binding energy for $5a_1$. The calculated intensities all agree that 1e is somewhat more intense. The experimental peak is asymmetric on the high binding energy side, indicating the location of the smaller peak. This is seen most clearly in Fig. 3. Thus, the Gelius model seems to favor placing 1e at a lower binding energy than $5a_1$.

## $CH_2F_2$

The $2b_1$ and $3a_1$ orbitals are reported here for the first time. The level ordering indicated by orbital energies is supported by the intensity ratios. The remaining peaks are shown in more detail in Fig. 3. In the case of the two lowest binding energy groups of peaks, our analysis of the peaks in Fig. 3 is based on the calculated CNDO intensities which give a good overall fit of the experimental data. The experimental ratio of the $1a_2$, $4b_1$, $6a_1$ peak area to that of the $2b_2$ peak is approximately 5:1. This is to be compared to a ratio of 3:1 in the He II spectrum[8]. The increase in the relative intensities over the statistical value can be understood in terms of our model as follows: the orbitals $1a_2$ and $4b_1$ do not have any hydrogen character by symmetry. The $6a_1$ has less contribution from hydrogen than does $2b_2$.[9] Thus, in all four orbitals most of the electron density is on the fluorines, mainly in the 2p levels; and the ($1a_2$ + $4b_1$ + $6a_1$) peak has a larger percentage of electrons on the fluorines than does $2b_2$.

In the next peak, at ~ 19 eV, there are three orbitals. The ordering of $3b_1$ and $5a_1$ may be reversed without disagreeing with our spectrum. However, it seems quite likely that $1b_2$ has a higher binding energy than both of them, as shown, because its low intensity is consistent with the asymmetry of this peak on the high-energy side.

## $CHF_3$

The *ab initio* and CNDO calculations, together with the Gelius model place $3a_1$ unambiguously as the most tightly bound MO. The model also seems to indicate that 3e is less tightly bound than $5a_1$ (Fig. 3). This is in agreement

with Brundle et al.[8] who relied on the Koopmans' theorem energies. We also propose in Fig. 3 an ordering for the four outer orbitals which is predicted by POLYATOM.[9] This fit was obtained using the reported UPS vertical ionization potentials and the area ratios calculated from CNDO. The ordering of $5e_1$ and $1a_2$ is reversed by CNDO. On the basis of intensity ratios our spectra establish the ordering of these four levels as shown in Fig. 3.

## $CF_4$

Siegbahn[16] has studied the $CF_4$ spectrum with monochromatized x-rays. His results as well as ours show that the least-bound orbital is more intense than the next one. According to the cross-section ratios obtained from both POLYATOM and CNDO/2 populations $1t_1$ should be the least-bound orbital (see Table III) as predicted by ab initio calculations. Thus comparision with our experimental intensities very slightly favors $1t_1$ as the most weakly bound orbital.

## V. TRENDS THROUGH THE SERIES

Some interesting binding-energy correlations can be made through the fluoromethane series. For example, Brundle et al.[8] noted that the energies of the $4a_1$ orbitals increase linearly with fluorination. These orbitals show strong C-H overlap (see Table III of Ref. 8). The total C-H overlap ($P_{C-H}$) of $4a_1$ is plotted against our experimental $4a_1$ binding energies in Fig. 4. For $CH_4$ the corresponding level is $2a_1$. Substitution of fluorines for hydrogens results in a migration of electron population from the C-H region toward the fluorines, thus increasing the $4a_1$ binding energies. At the same time, the populations of the remaining C-H bonds are left essentially intact. Additivity of inductive effects in the fluoromethanes and other compounds has been observed elsewhere.[17]

The $3a_1$ orbital is C-F bonding and a plot of total overlap populations[9] versus $3a_1$ binding energy is also shown in Fig. 4. The C-F bonding population for a single bond decreases through the series $CH_3F \rightarrow CF_4$, but the total bonding population shows an almost linear increase with the binding energy of the $3a_1$ orbital.

The $2b_1$ level of $CH_2F_2$, 2e of $CHF_3$ and $2t_2$ of $CF_4$ can be grouped together. The variation in their binding energies, which increase by 1 eV for the substitution of a hydrogen by a fluorine, correlates linearly with the F 2s populations (gross or net) of these orbitals. This is shown in Table IV.

These linear relationship extend the concept of "group shifts", which could be expressed by the relation[18]

$$\Delta E = \sum_{\text{group}} (\Delta E_{\text{group}} - \Delta E_H) \ .$$

Furthermore, the point-charge potential concepts that led to this equation for core levels is clearly not viable here: the slopes $\Delta E(Cls)/\Delta E(4a_1)$ are not compatible with such a model, for example. Bond energies would have to be explicitly taken into account to explain the slopes in Fig. 4. Further interpretation of these linear relationships would be outside the scope of this paper. We wish simply to note their existence and to observe that they are consistent with chemical intuition.

FOOTNOTES AND REFERENCES

*Work performed under the auspices of the U. S. Atomic Energy Commission.

1. D. W. Turner, C. Baker, A. D. Baker and C. R. Brundle, Molecular Photoelectron Spectroscopy (Wiley-Interscience, London, 1970).

2. K. Siegbahn, C. Nordling, G. Johansson, J. Hedman, P. F. Heden, K. Hamrin, U. Gelius, T. Bergmark, L. O. Werme, R. Manne and Y. Baer, ESCA Applied to Free Molecules (North Holland, Amsterdam, 1969).

3. U. Gelius in Electron Spectroscopy, D. A. Shirley, ed., (North-Holland, Amsterdam, 1972).

4. R. S. Mulliken, J. Chem. Phys. 23, 1833 (1955).

5. D. W. Davis, D. A. Shirley, and T. D. Thomas, J. Amer. Chem. Soc. 94 , 6565 (1972).

6. A neon 2s value of 48.47 eV has been reported recently. See G. Johansson, J. Hedman, A. Berndtsson, A. Klasson and R. Nilsson, J. Electr. Spectr. 2, 295 (1973).

7. C. R. Brundle, Chem. Phys. Letters 7, 317 (1970)

8. C. R. Brundle, M. B. Robin and H. Basch, J. Chem. Phys. 53, 2196 (1970).

9. L. C. Snyder and H. Basch, Molecular Wave Functions and Properties (John Wiley and Sons, New York, 1972).

10. T. Koopmans, Physica 1, 104 (1933).

11. P. S. Bagus, Phys. Rev. 139, A619 (1965).

12. D. A. Shirley, Chem. Phys. Letters 16, 220 (1972).

13. D. W. Davis and D. A. Shirley, Chem. Phys. Letters 15, 185 (1972).

14. (a) S. P. Kowalczyk, R. A. Pollak, F. R. McFeely, L. Ley, and D. A. Shirley, Phys. Rev. B 8, 2387 (1973).

(b) L. Ley, S. P. Kowalczyk, F. R. McFeely, R. A. Pollak and D. A. Shirley, Phys. Rev. B, 8, 2392 (1973).

15. See for example C. A. Coulson and H. L. Strauss, Proc. Roy. Soc. (London) A 269, 443 (1962), and ref. 8.

16. K. Siegbahn, in Atomic Physics 3, Proceedings of the Third International Conference on Atomic Physics, Boulder, Colorado, 1972, edited by S. J. Smith and G. K. Walters, p. 493. Also K. Siegbahn, University of Uppsala, Report No. UUIP-793.

17. D. W. Davis, M. S. Banna and D. A. Shirley, J. Chem. Phys. 60, 237 (1974).

18. D. A. Shirley, in Advances in Chemical Physics, Vol. 23 (I. Prigogine and Stuart A. Rice, editors), p. 85 (1973).

Table I. Molecular Orbital Binding Energies in Fluorinated Methanes (in eV).

| Molecule | Orbital | $E_B$(XPS)[a] | $E_B$(UPS)[b] | $-\varepsilon_{ab\ initio}$ | $-\varepsilon_{CNDO/2}$ | $\Delta\varepsilon_{ai}$ | $E_B$(theo) |
|---|---|---|---|---|---|---|---|
| $CH_4$ | $1t_2$ | 14.2(2)[c] | 14.0 | 14.74 | 19.79 | 0.6 | 13.74 |
| | $2a_1$ | 23.05(2) | 23.0 | 25.68 | 34.54 | 2.63 | 24.68 |
| $CH_3F$ | 2e | 13.31(4) | 13.05 | 14.43 | 17.57 | 1.12 | 12.93 |
| | 1e | 16.85(7) | ~17.0 | 18.00 | 21.28 | 1.15 | 16.50 |
| | $5a_1$ | 17.56(9) | | 18.89 | 24.12 | 1.33 | 17.39 |
| | $4a_1$ | 23.48(3) | 23.4 | 26.13 | 32.06 | 2.65 | 24.63 |
| | $3a_1$ | 38.41(3) | - | 43.17 | 47.10 | 4.76 | 38.17 |
| $CH_2F_2$ | $2b_2$ | 13.17[d,e] | 13.27 | 14.89 | 17.11 | 1.72 | 12.89 |
| | $6a_1$ | 14.91[e] | | 16.94 | 18.88 | 2.03 | 14.94 |
| | $4b_1$ | 15.20[d,e] (2) | 15.3 | 17.23 | 19.82 | 2.03 | 15.23 |
| | $1a_2$ | 15.61[d,e] | 15.71 | 18.22 | 21.38 | 2.61 | 16.22 |
| | $3b_1$ | 18.51(4)[e] | | 20.38 | 23.96 | 1.87 | 18.38 |
| | $5a_1$ | 19.07(3)[e] | 18.9 | 21.13 | 25.23 | 2.06 | 19.13 |
| | $1b_2$ | 19.76(7) | | 21.54 | 26.97 | 1.78 | 19.54 |
| | $4a_1$ | 23.86(3) | 23.9 | 26.77 | 31.15 | 2.91 | 24.77 |
| | $2b_1$ | 38.20(7) | - | 43.79 | 45.82 | 5.59 | 38.29 |
| | $3a_1$ | 40.13(7) | - | 45.63 | 50.15 | 5.50 | 40.13 |
| $CHF_3$ | $6a_1$ | 14.67[d,e] | 14.80 | 16.53 | 17.77 | 1.86 | 14.03 |
| | $1a_2$ | 15.29[d,e] | 15.5 | 18.33 | 21.52 | 3.04 | 15.83 |
| | 5e | 15.99[d,e] (4) | 16.2 | 18.54 | 19.94 | 2.55 | 16.04 |
| | 4e | 17.03[d,e] | 17.24 | 19.71 | 22.24 | 2.68 | 17.21 |

(continued)

Table I. (continued)

| Molecule | Orbital | $E_B$(XPS)[a] | $E_B$(UPS)[b] | $-\varepsilon_{ab\ initio}$ | $-\varepsilon_{CNDO/2}$ | $\Delta\varepsilon_{ai}$ | $E_B$(theo |
|---|---|---|---|---|---|---|---|
| | 3e | 20.25(3) | 20.6[f] | 22.87 | 26.35 | 2.62 | 20.37 |
| | $5a_1$ | 20.89(3) | | 23.78 | 27.86 | 2.89 | 21.28 |
| | $4a_1$ | 24.38(3) | 24.44 | 27.49 | 30.88 | 3.11 | 24.99 |
| | 2e | 39.15(4) | - | 45.34 | 47.20 | 6.19 | 39.34 |
| | $3a_1$ | 42.03(9) | - | 48.22 | 52.78 | 6.19 | 42.22 |
| $CF_4$ | $1t_1$ | 16.23(3) | 16.20 | 19.40 | 22.24 | 3.17 | 16.40 |
| | $4t_2$ | 17.41(4) | 17.40 | 19.65 | 20.20 | 2.24 | 16.65 |
| | 1e | 18.43(4) | 18.50 | 21.34 | 23.30 | 2.91 | 18.34 |
| | $3t_2$ | 22.14(2) | 22.12 | 24.89 | 28.18 | 2.75 | 21.89 |
| | $4a_1$ | 25.11(2) | 25.12 | 28.15 | 29.48 | 3.04 | 25.15 |
| | $2t_2$ | 40.30(4) | - | 46.65 | 48.22 | 6.35 | 40.15 |
| | $3a_1$ | 43.81(10) | - | 50.50 | 54.63 | 6.69 | 44.00 |
| HF | $1\pi$ | 16.12(4) | 16.04 | 17.50 | 21.28 | | |
| | $3\sigma$ | 19.89(7) | 19.90 | 20.50 | 23.14 | | |
| | $2\sigma$ | 39.65(2) | - | 43.61 | 45.55 | | |

[a] Binding energies using Mg Kα x-rays except with $CH_4$ where Al Kα x-rays were used.

[b] Vertical binding energies from Ref. 8.

[c] Weighted average of Jahn-Teller levels

[d] Separations from UPS used.

[e] Area ratios from CNDO/2 used.

[f] This value is probably correct. The value given in Ref. 8 is 19.84 eV for the vertical IP and 20.6 eV for the adiabatic IP.

Table II. Calculated Relative Atomic Photoelectric Cross Sections.

| Ratio | CNDO | POLYATOM(Net)[b] | POLYATOM (Gross)[b] | Gelius[a] |
|---|---|---|---|---|
| $\sigma$(C2s)/$\sigma$(C2p) | 23.3[c] | 19.9 | 12.6[c] | 13 |
| $\sigma$(F2s)/$\sigma$(F2p) | 9.5[d] | 10.3[d] | 9.1[d] | 10 |
| $\sigma$(F2s)/$\sigma$(C2s) | 8.0[e] | 5.8[e] | 3.5[e] | 2 |

[a] Ref. 3.

[b] Wavefunctions and overlaps obtained from Ref. 9.

[c] Using relative areas of $2a_1$ and $1t_2$ orbitals of methane.

[d] Using relative areas of $2\sigma$ and $1\Pi$ orbitals of hydrogen fluoride

[e] Using relative areas of $3a_1$ and $4a_1$ orbitals of methyl fluoride.

Table III. Computed Molecular Orbital Intensity Ratios from CNDO and POLYATOM Calculations.

| Molecule | Molecular Orbital | $I^{a}_{CNDO}$ | $I^{b}_{NP}$ | $I^{c}_{GP}$ | $I_{exp}$ | |
|---|---|---|---|---|---|---|
| HF | $1\pi$ | 0.24 | 0.24 | 0.24 | 0.24(2) | |
| | $3\sigma$ | 0.14 | 0.20 | 0.16 | 0.19(3) | |
| | $2\sigma$ | 1.00 | 1.00 | 1.00 | 1.00(2) | |
| $CH_4$ | $1t_2$ | 0.12 | 0.12 | 0.12 | 0.12[d](2) | |
| | $2a_1$ | 1.00 | 1.00 | 1.00 | 1.00(3) | |
| $CH_3F$ | 2e | 0.14 | 0.12 | 0.11 | 0.13(1) | |
| | 1e | 0.14 | 0.14 | 0.15 | 0.11(2) | |
| | $5a_1$ | 0.12 | 0.11 | 0.11 | 0.08(2) | |
| | $4a_1$ | 0.24 | 0.23 | 0.26 | 0.23(1) | |
| | $3a_1$ | 1.00 | 1.00 | 1.00 | 1.00(3) | |
| $CH_2F_2$ | $2b_2$ | 0.058 | 0.064 | 0.065 | 0.05[e,f] | (1) |
| | $6a_1$ | 0.089 | 0.10 | 0.11 | 0.07[e] | (1) |
| | $4b_1$ | 0.11 | 0.12 | 0.11 | 0.09[e,f] | (1) |
| | $1a_2$ | 0.12 | 0.12 | 0.12 | 0.09[e,f] | (1) |
| | $3b_1$ | 0.14 | 0.16 | 0.15 | 0.08[e] | (1) |
| | $5a_1$ | 0.14 | 0.10 | 0.11 | 0.08[e] | (1) |
| | $1b_2$ | 0.062 | 0.055 | 0.063 | 0.04[e] | (1) |
| | $4a_1$ | 0.24 | 0.32 | 0.33 | 0.28(1) | |
| | $2b_1$ | 1.00 | 1.00 | 1.00 | 1.00(6) | |
| | $3a_1$ | 0.84 | 0.85 | 0.90 | 0.89(5) | |

(continued)

Table III. (continued)

| Molecule | Moleculear Orbital | $I^{a}_{CNDO}$ | $I^{b}_{NP}$ | $I^{c}_{GP}$ | $I_{exp}$ |
|---|---|---|---|---|---|
| $CHF_3$ | $6a_1$ | 0.038 | 0.049 | 0.042 | 0.03[e,f] } (1) |
| | $1a_2$ | 0.062 | 0.064 | 0.071 | 0.05[e,f] } (1) |
| | 5e | 0.12 | 0.12 | 0.12 | 0.09[e,f] } (1) |
| | 4e | 0.12 | 0.12 | 0.13 | 0.09[e,f] } (1) |
| | 3e | 0.18 | 0.19 | 0.20 | 0.09(1) |
| | $5a_1$ | 0.12 | 0.048 | 0.052 | 0.06(1) |
| | $4a_1$ | 0.10 | 0.20 | 0.15 | 0.18(1) |
| | 2e | 1.00 | 1.00 | 1.00 | 1.00(3) |
| | $3a_1$ | 0.43 | 0.40 | 0.48 | 0.42(2) |
| $CF_4$ | $1t_1$ | 0.13 | 0.14 | 0.14 | 0.12(1) |
| | $4t_2$ | 0.12 | 0.13 | 0.12 | 0.11(1) |
| | 1e | 0.083 | 0.080 | 0.086 | 0.08(1) |
| | $3t_2$ | 0.20 | 0.23 | 0.23 | 0.17(1) |
| | $4a_1$ | 0.11 | 0.16 | 0.12 | 0.16(1) |
| | $2t_2$ | 1.00 | 1.00 | 1.00 | 1.00(3) |
| | $3a_1$ | 0.28 | 0.26 | 0.31 | 0.29(2) |

[a] Relative intensity using CNDO populations.

[b] Relative and intensity using POLYATOM net populations calculated from ref. 9.

[c] Relative intensity using POLYATOM gross populations calculated from ref. 9.

[d] Assuming one level, not Jahn-Teller split.

[e] Area ratios taken from CNDO.

[f] Separations taken from UPS.

Table IV. F2s Binding Energies and Populations for the Next-To-Innermost Molecular Orbital of $CH_2F_2$, $CHF_3$ and $CF_4$.

| Molecule | Orbital | Binding Energy(eV) | Gross Population* | Net Population* |
|---|---|---|---|---|
| $CH_2F_2$ | $2b_1$ | 28.20 | 1.84 | 1.22 |
| $CHF_3$ | 2e | 39.19 | 3.48 | 2.36 |
| $CF_4$ | $2t_2$ | 40.18 | 5.07 | 3.45 |

*Calculated from ref. 9.

FIGURE CAPTIONS

Fig. 1. X-ray photoelectron spectra of HF and the fluoromethane series $CH_{4-n}F_n$ ($0 \leqslant n \leqslant 4$) taken at increments of $\sim$ 0.33 eV. Vertical bars correspond to intensity ratios computed using POLYATOM net populations.[9] They are not corrected for the considerable variation in line width. In some cases, noted in Table I, separations from UPS and/or intensity ratios from CNDO/2 were used. For $CH_2F_2$ two groups of levels were fit as two peaks.

Fig. 2. Plot of binding energies calculated from a three-parameter model versus experimental values.

Fig. 3. X-ray photoelectron spectra of the fluoromethanes in the region up to approximately 30 eV binding energy taken at increments of $\sim$ 0.16 eV. Vertical bars correspond to computed intensity ratios using CNDO/2 populations. In some cases separations and intensity ratios were used as explained for Fig. 1.

Fig. 4. Variation of total C-F overlap population of $3a_1$ and total C-H overlap population of $4a_1$ ($2a_1$ in methane) with binding energies of $3a_1$ and $4a_1$ respectively. Overlap populations were obtained from refs. 8 and 9.

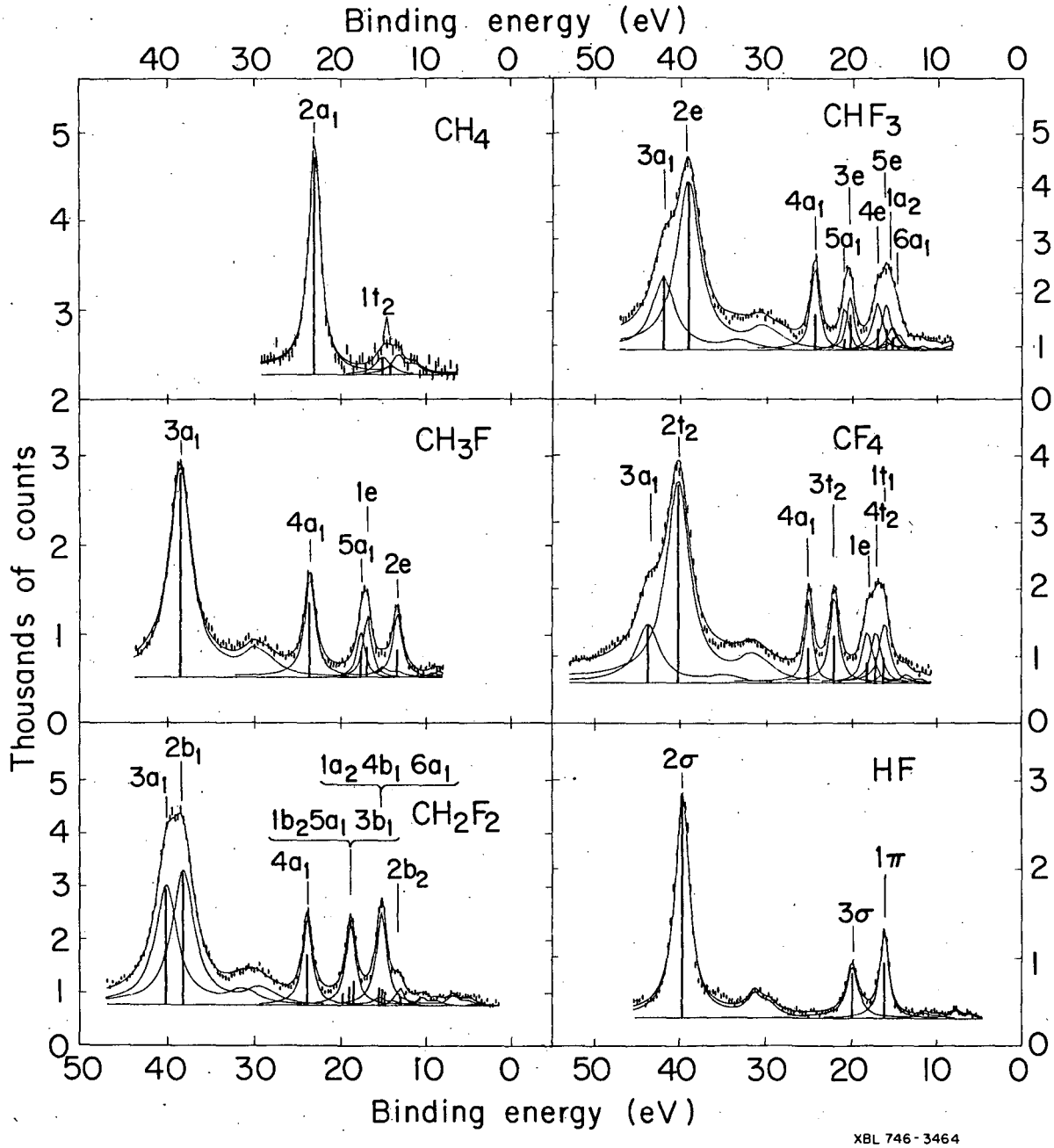
Binding energy (eV)
Thousands of counts
2a1
1t2
CH4
2e
3a1
4a1
3e
5e
5a1
4e
1a2
6a1
CHF3
3a1
4a1
5a1
1e
2e
CH3F
2t2
3a1
3t2
1t1
4a1
4t2
1e
CF4
2b1
3a1
1a2 4b1 6a1
1b2 5a1 3b1
4a1
2b2
CH2F2
2σ
1π
3σ
HF
XBL 746-3464

Fig. 1

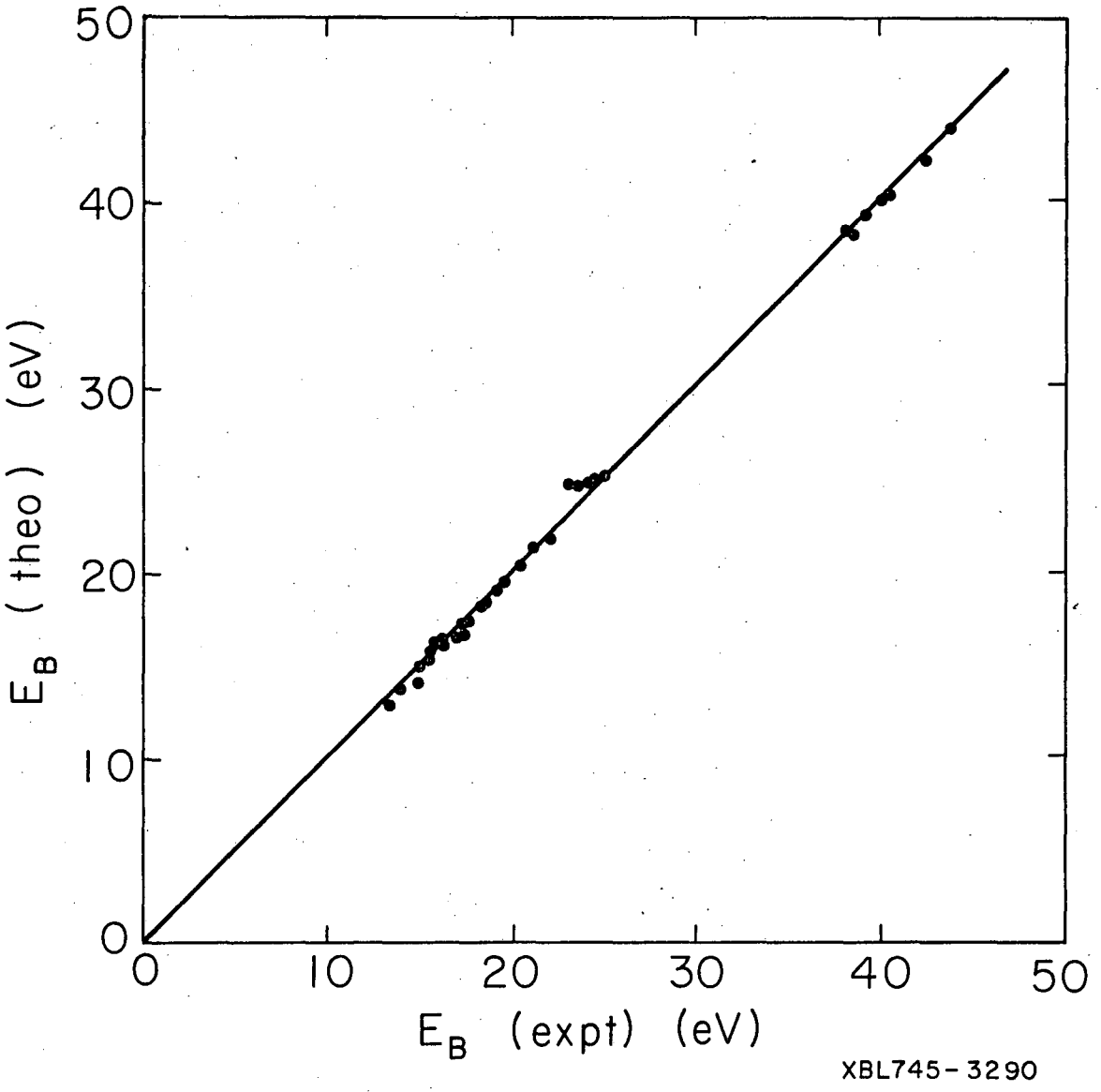


Fig. 2

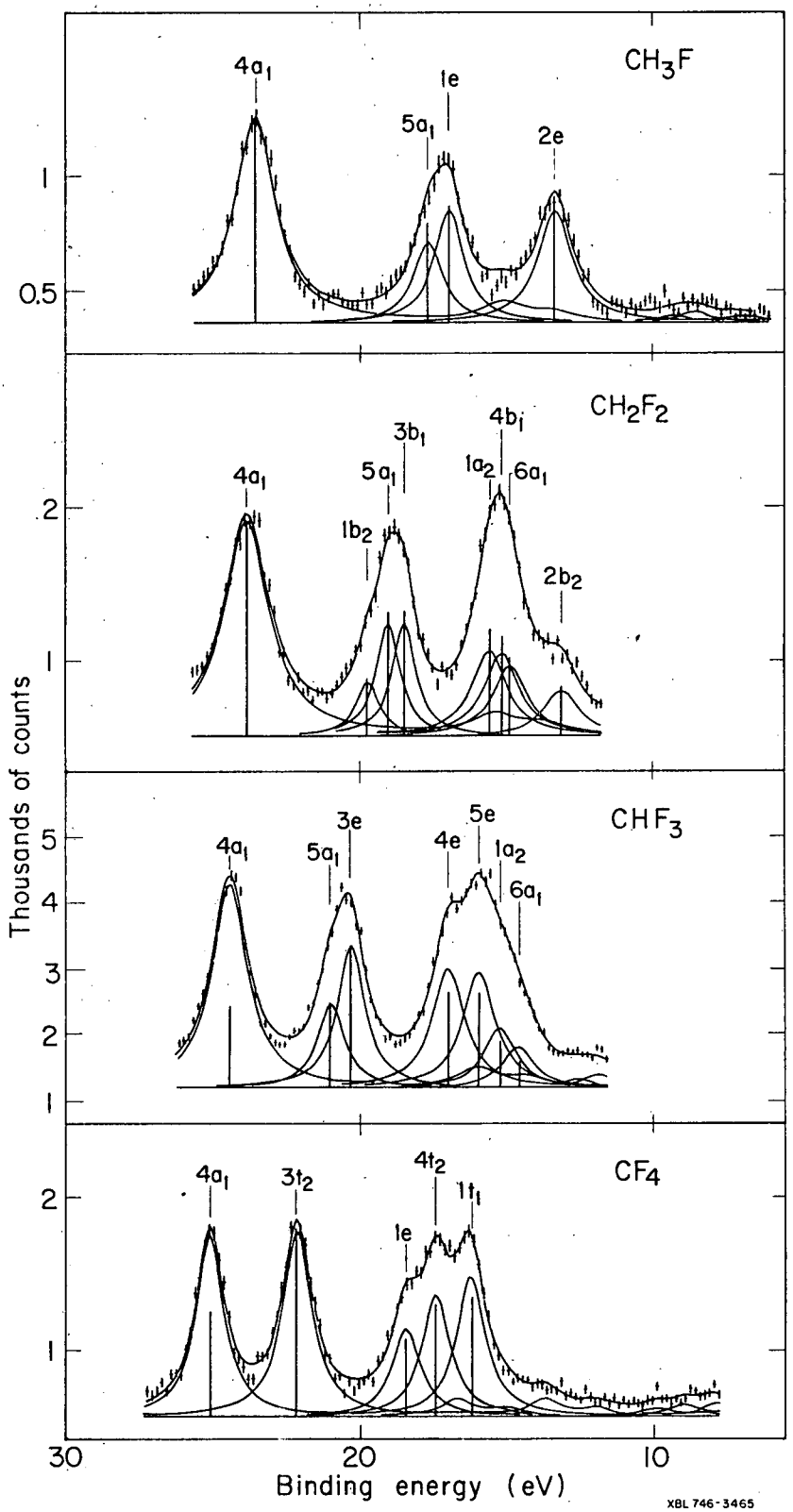
CH3F
4a1
1e
5a1
2e
CH2F2
4a1
3b1
5a1
4b1
1a2
6a1
1b2
2b2
CHF3
4a1
5a1
3e
4e
5e
1a2
6a1
CF4
4a1
3t2
4t2
1t1
1e
Thousands of counts
Binding energy (eV)
30
20
10
XBL 746-3465

Fig. 3

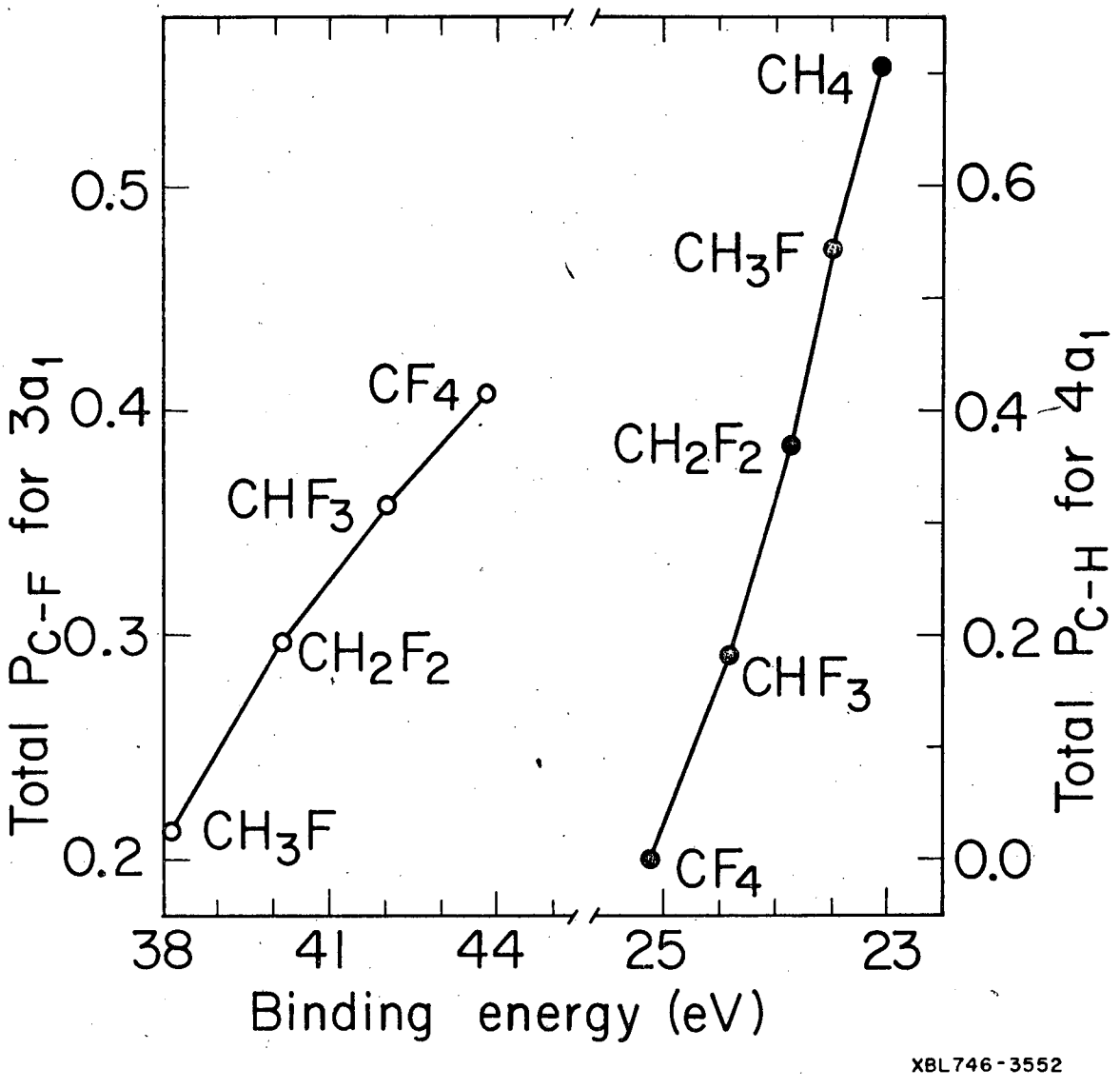
CH4
CH3F
CH2F2
CHF3
CF4
CF4
CHF3
CH2F2
CH3F
0.5
0.4
0.3
0.2
0.6
0.4
0.2
0.0
38
41
44
25
23
Binding energy (eV)
Total Pc-F for 3a1
Total Pc-H for 4a1
XBL746-3552

Fig. 4

*TECHNICAL INFORMATION DIVISION*
*LAWRENCE BERKELEY LABORATORY*
*UNIVERSITY OF CALIFORNIA*
*BERKELEY, CALIFORNIA 94720*